Heliyon

ELSEVIER

Received:
29 July 2018
Revised:
31 October 2018
Accepted:
3 December 2018

Cite as: Rabie Kachkoul, Tarik Sqalli Houssaini, Radouane El Habbani, Youssef Miyah, Mohamed Mohim, Anissa Lahrichi. Phytochemical screening and inhibitory activity of oxalocalcic crystallization of *Arbutus unedo* L. leaves. Heliyon 4 (2018) e01011. doi: 10.1016/j.heliyon.2018.e01011

Phytochemical screening and inhibitory activity of oxalocalcic crystallization of *Arbutus unedo* L. leaves

Rabie Kachkoul [a,*], **Tarik Sqalli Houssaini** [b,c], **Radouane El Habbani** [a], **Youssef Miyah** [a], **Mohamed Mohim** [c], **Anissa Lahrichi** [a]

[a] *Laboratory of Biochemistry, Faculty of Medicine and Pharmacy, University Sidi Mohammed Ben Abdellah, BP 1893, Km 22, Road of Sidi Harazem, Fez, Morocco*

[b] *Department of Nephrology, University Hospital Hassan II, BP 1835, Atlas, Road of Sidi Harazem, Fez, Morocco*

[c] *Laboratory of Molecular Bases in Human Pathology and Therapeutic Tools, Faculty of Medicine and Pharmacy, University Sidi Mohammed Ben Abdellah, BP 1893, Km 22, Road of Sidi Harazem, Fez, Morocco*

[*] Corresponding author.

E-mail address: rabie.kachkoul@usmba.ac.ma (R. Kachkoul).

Abstract

The present study is focused on the experimental verification of the efficiency of *Arbutus unedo* L. leaves against the crystallization of calcium oxalate. The inhibition of crystallization has been studied in vitro with the absence and the presence of the different concentrations of the infusion and hydroalcoholic extract of the plant. This study consists of measuring, using a UV-Visible spectrophotometer, the temporal evolution of the optical density at $\lambda = 620$ nm corresponding to the crystals formation. The latter have been characterized by microscopic observation using an optical microscope, and by Fourier Transform Infrared Spectroscopy (FT-IR). The results suggest a greater effectiveness of the plant infusion with respect to the hydroalcoholic extract against crystallization or nucleation at percentages of 69.41 ± 0.24 or 19.76 ± 0.27% and at 93.92 ± 2.61 and 45.16 ± 3.06% against the aggregation, for both the infusion and the hydroalcoholic extract respectively. *A. unedo* leaves is a very promising and

https://doi.org/10.1016/j.heliyon.2018.e01011

effective remedy against the crystallization of calcium oxalate and especially in the aggregation stage.

Keywords: Biochemistry, Pharmaceutical science, Plant biology

1. Introduction

Urolithiasis is a pathological disease coming from a urinary biochemical imbalance characterized by the formation of stones in the kidneys or in the urinary tract. In this case, the disease represents a multifactorial etiology in terms of factors: anatomical, environmental, genetic, infectious, metabolic, nutritional and equally important socio-economic factors [1]. Besides, the study of the epidemiological profile reveals that the lithiasis affects 4% to 20% of the population, with a recurrence rate estimated at 50% during the first 5 years and thus the predominant stone have the chemical composition majority calcium oxalate [2, 3, 4, 5, 6, 7]. Additionally, calcium oxalate crystals are found mainly in three different forms namely: calcium oxalate monohydrate (COM) called Whewellite, calcium oxalate dihydrate (COD) or Weddellite and oxalate calcium trihydrate (COT). COM form is the most stable thermodynamically and the most common ingredient of stone with a higher affinity for both renal tubular cells. Therefore it is responsible for the formation of stones in the kidney [8, 9].

Currently medical management of urolithiasis involves medical treatments and/or surgical procedures for the stones extraction with techniques such as: extracorporeal lithotripsy, ureteroscopy, percutaneous nephrolithotomy and open surgery. These methods can lead to side effects such as hemorrhage, hypertension, tubular necrosis and subsequent fibrosis of the kidney [1], Thereforethe research for prevention methods against crystallization is a promising path to explore preventing a possible recurrence in patients. In Morocco the use of alternative methods, addressing medicinal and aromatic plants (MAP) is widely spread resulting many ethnobotanical studies carried out by different researchers that have shown the effectiveness of the latter in the treatment of lithiasis aiming to expel and prevent the recurrence of stones as well as to relieve renal colic [10, 11, 12, 13].

A. unedo is a plant widely used in traditional medicine for the treatment of diseases including renal diseases [14], cardiovascular, gastrointestinal, dermatological and urological disorders [15]. However, several *in vivo* and *in vitro* studies have been reported of the very important biological activities of the plant: delayed development of hypertension, improvement of cardiovascular and renal functions in rats [16, 17], also endothelial vasorelaxation on the isolated rat aorta [18], as well as a high antioxidant and antibacterial capacity [19], and an interesting anti-inflammatory activity [20]. It is a typical evergreen, sclerophytic, species of Mediterranean vegetation

https://doi.org/10.1016/j.heliyon.2018.e01011

member of Ericaceae family [21]. In this context, the aim of this study was to evaluated *in vitro* the capacity of the two *A. unedo* leaf extracts: infusion and hydroalcoholic extract in the inhibition of calcium oxalate crystallization, as well as, to carry out a phytochemical screening and to determine the total phenolic content in the plant.

2. Materials and methods

2.1. Extraction

2.1.1. Hydroethanoic extract

Plant material collected from the mature individuals *A. unedo* in a single harvest site in the Taounate region (located in the north of Morocco, 92 km from the city of Fez, 34° 32′ 09 ″N, 4° 38′ 24″ W), in March 2017. After species identification, the leaves were dried at room temperature (25 °C), in the dark, and minced to obtain a fine fraction. The preparation of the hydroalcoholic extract (E.FA) consists in introducing 20 g of leave-powder, in the cellulosic cartridge; the latter is inserted into the extractor of the Soxhlet assembly, which is surmounted by a refrigerant and 170 ml of n-hexane in the mounting flask, following boiling for 4 h at 65 °C. The lipid extract is then recovered by removing the solvent contained in the distillation flask using a rotary vacuum evaporator [22, 23]. A second hydroalcoholic extraction is carried out on the defatted mark in the same way as the first extraction, using a mixture of ethanol/distilled water (80:20 v:v) for 4 h. Moreover, elimination of ethanol and water is also done with the rotavapor at 40 °C.

2.1.2. Infusion

The infusion was prepared by the method described by Jiménez-Zamora *et al.* [24] with some modifications. 2 g of *A. unedo* leaves-powder, placed in a volume of 100 ml of boiling distilled water, is allowed to be infused for 30 min, then filtered using a filter paper of 1.6 μm diameters. The infusion obtained was stored in a temperature of −20 °C until use.

2.2. Phytochemical screening

This is a qualitative analytical study which aims to find the main chemical groups in the studied plant, these are tests based on visual observation of the color change and/or the formation of precipitates after the addition of a specific reagent. For this reason, initial solutions were prepared with concentrations of: for I.FA, 5 g of the powder of the plant infused in 1 liter boiling distilled water, for E.FA, 4g of extract solubilised in 100 ml distilled water.

https://doi.org/10.1016/j.heliyon.2018.e01011

2.2.1. Polyphenols test

A drop of alcoholic solution of 2% ferric chloride was added to 2 ml of the extract. The appearance of a more or less dark blue-blackish or green coloration was a sign of the polyphenols presence [25].

2.2.2. Flavonoids test

A few drops of concentrated hydrochloric acid and 2−3 magnesium chips were added to 5 ml of the extract that had been placed in a test tube. The release of heat and the emerge of a pink-orange or purplish color indicated the presence of flavonoids [26].

2.2.3. Tannins test

In a test tube containing 5 ml of the extract, 15 ml of Stiasny's reagent was added. The mixture was kept in a bain-marie at 80 °C for 30 min. The appearance of a precipitate in large flakes characterized the catechin tannins. As for the gallic tannins, we have a filtration of the previous solution. The filtrate is saturated with sodium acetate and then the addition of 3 drops of $FeCl_3$, the appearance of an intense blue-black color reveals the presence of gallic tannins [25].

2.2.4. Saponins test

10 ml of distilled water were added to 5 ml of the extract in a test tube. After that, it is stirred for 20 sec and allowed to stand for 15 min. Hence, the appearance of foam of height higher than 1 cm and its persistence indicated the presence of saponins [26].

2.2.5. Sterols and polyterpenes tests

1 ml of acetic anhydride, 0.5 ml of chloroform and 0.5 ml of concentrated sulfuric acid without stirring were added to 5 ml of the extract in a test tube. The appearance, at the interphase, of a purple or purple ring, turning blue then green, indicates the presence of both sterols and polyterpenes [27].

2.2.6. Alkaloids test

Alkaloids are characterized by the use of Mayer's and Wagner's reagents [28]. The principle is, to first, prepare a chloridic extract from 15 mg of extract and 5 ml of 1% HCl which is heated for 5 min in a bath and then filtered on filter paper. Then, the filtrate is put in two test tubes in which a few drops of Mayer's reagent in the first tube and a few drops of Wagner's reagent in the second tube are added. The appearance of yellowish-white precipitate (Mayer) and a brown-red precipitate (Wagner) denoted the presence of alkaloids [29].

https://doi.org/10.1016/j.heliyon.2018.e01011

2.3. Total polyphenols content determination

The total polyphenol content was determined by the Folin-Ciocalteu reagent according to the method of Singleton and Rossi [30] with some modifications: 100 μl of the extract is mixed with 500 μl of Folin-Ciocalteu reagent (diluted 10 times in distilled water) and enabled to stand at room temperature for 5 min. Then 750 μl of the Na_2CO_3 solution (60 gl^{-1}) is added. Additionally, absorbance is measured at 760 nm after 90 min of incubation in the dark. Further, a standard calibration curve of gallic acid (0 to 0.2 mg/ml) is prepared and the outcomes are expressed in mg gallic acid equivalent (GAE) per g of dry leaves (mg/g) [31].

2.4. Inhibition of the calcium oxalate's crystallization

The inhibition of the crystallization has been studied according to the protocol described by Hess *et al.* [32]. In this respect, stock solutions of $CaCl_2$:$2H_2O$ (15 mM) and $Na_2C_2O_4$ (1.5 mM) containing 200 mM NaCl have been prepared to which 10 mM sodium acetate has been added to adjust the pH value to 5.7. Before being used in crystallization experiments, the solutions have been filtered through filters having a pore diameter of 0.22 μm and reheated to 37 °C. On the other hand, for crystallization experiments without inhibitor, 1.5 ml of the $CaCl_2$: $2H_2O$ solution has been transferred to a quartz cuvette optical path 10 mm. Besides, an identical volume of the $Na_2C_2O_4$ solution has been added to trigger crystal formation and corresponds to "t" equal to zero. Thus, final concentrations test are 5 mM and 0.5 mM calcium and oxalate respectively with a calcium/oxalate concentration ratio equal to 10 which corresponds to whewellite formation.

The temporal measurements of the optical density "OD" have been recorded over a period of one hour: every 15 s for the first ten min and every thirty s thereafter. All the crystallization experiments took place using a UV-Visible spectrophotometer at the wavelength λ equal to 620 nm which corresponds to the detection of the crystals. Similarly, the same experiments have been accomplished with several concentrations of 0.5; 1 and 2 gl^{-1} of the hydroalcoholic extract and 1, 3 and 6 gl^{-1} of the infusion. The experiments have been carried out with 1 ml $CaCl_2$:H_2O and 1 ml of the extract to which 1 ml $Na_2C_20_4$ is added which promotes the formation of crystals. Hence, all experiments have been performed three times.

The slopes of the nucleation phase "SN" and aggregation "SA", has been calculated using linear regression analysis. Indeed, the maximum slope of increase of OD as a function of time corresponds mainly to the nucleation phase "SN" which means the increase of the number of particles. Subsequently, a gradual decrease in OD with time is both observed and corresponds to the decrease in the number of crystals

https://doi.org/10.1016/j.heliyon.2018.e01011

due to their aggregations [33]. The maximum slope of the OD decrease as a function of time has a negative value. For convenience, a positive number for the aggregation slope "SA" will be used for all comparisons.

The percentages of inhibitions have been calculated by the relation of Hess et al. [32,34].

% Nucleation inhibition: $[1-(SNi/SNs)] \times 100$

% Aggregation inhibition: $[1-(SAi/SAs)] \times 100$

where "i" and "s" represent tests with and without inhibitor respectively. The correlation coefficient (R) and the coefficient of variation (CV) are calculated to verify the validity of our results.

2.5. Microscopic observation

The microscopic observation of the crystals in the liquid phase has been carried out using a polarized optical microscope equipped with a photon-numeric apparatus and connected to a computer.

2.6. Characterization of crystals

The characterization and the determination of the chemical composition have been made by Fourier Transform Infrared Spectroscopy (FT-IR) between 4000 and 400 cm^{-1} with a resolution of 4 cm^{-1}, on crystals synthesized in the absence and presence of both inhibitors. In fact, on a volume V of a $CaCl_2$: $2H_2O$ (15 mM) solution, the same volume of inhibitor and the solution of $Na_2C_2O_4$ (1.5 mM) are added. The mixture is stirred continuously for half an hour, and then the solution is left to stand for 1 hour at 37 °C. Thereafter, the crystals were washed with ethanol 3 times and centrifuged at 4000 rpm and dried.

2.7. Statistical analysis

The data are expressed as mean ± SD of the three replicates, statistically analyzed and linear regression, has been performed using ANOVA One-Way Analysis followed by the Tukey multiple comparison test using Minitab 17, the p-value <0.05 is considered as significant.

3. Results

The yield of the hydroalcoholic extract leaves of *A. unedo*, obtained by the soxhlet extraction method compared to the initial dry matter is 20 ± 3.4%.

https://doi.org/10.1016/j.heliyon.2018.e01011

3.1. Phytochemical screening

Both the preliminary phytochemical screening of the hydroalcoholic extract (E.FA) and infusion (I.FA) of *A. unedo* leaves reveal the presence of different chemical families (Table 1), containing polyphenols and tannins at very high concentrations for both E.FA and I.FA. This is observed following the intense coloration caused by the strong reaction between sample and reagents. On the other hand, flavonoids, have been detected at moderate concentrations. However, the test showed the presence of sterols and polyterpenes traces in E.FA and a complete absence of these in I.FA while alkaloids and saponins are absent in both extracts of the plant similar to Mrabti *et al.* [35].

3.2. Total polyphenol content

Phenolic compounds have been quantified in the I.FA and E.FA of the plant (Fig. 1) and the total polyphenol contents varied between different extraction methods. In this case, analysis of the histogram reveals a higher content of polyphenols in I.FA compared to E.FA with amounts of 95.83 ± 2.083 and 22.13 ± 1.57 mg EAG/g of dry leaves, respectively. This indicates that the infusion method is the most suitable for the extraction of polyphenols.

3.3. Temporal evolution of the optical density

The analysis of the curve shape of the temporal evolution of the optical density in the presence of inhibitors of E.FA, I.FA and Potassium Citrate (Cit.K) taken as positive control (Fig. 2), display the presence of a weak slope of turbidity in the nucleation phase compared to that obtained in the absence of inhibitor (SI). This meant an impediment of the formation of crystalline nuclei especially in the presence Cit.K which remains more effective than the two plant extracts. For the aggregation phase, the I.FA has a very low turbidity slope that SI follows by Cit.K. On the other hand, E.FA shows a slightly weak slope. These explicit results well explain the superior

Table 1. Phytochemical screening of *A. unedo* leaves.

Phytochemical groups	I.FA	E.FA
Polyphenols	+++	+++
Flavonoids	++	++
Tannins	+++	+++
Saponins	-	-
sterols and polyterpenes	-	+
Alcaloides	-	-

+++: Very abundant, ++: abundant, +: medium, -: absence.
E.FA: hydroalcoholic extract of *A. unedo*, I.FA: infusion of *A. unedo*.

https://doi.org/10.1016/j.heliyon.2018.e01011

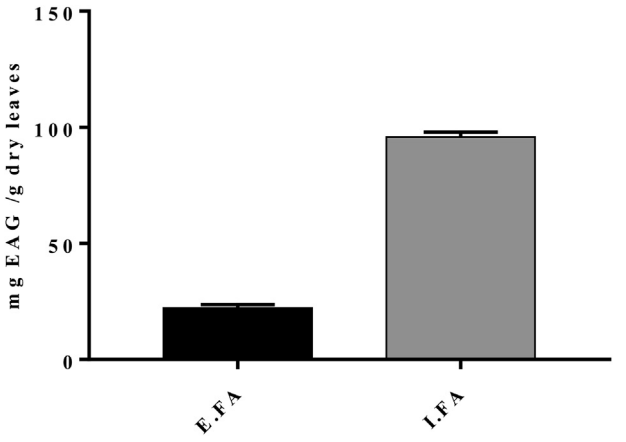

Fig. 1. Polyphenols contents in the I.FA and E.FA of the plant. Values are expressed as mean ± SD (n = 3). E.FA: hydroalcoholic extract of *A. unedo*, I.FA: infusion of *A. unedo*.

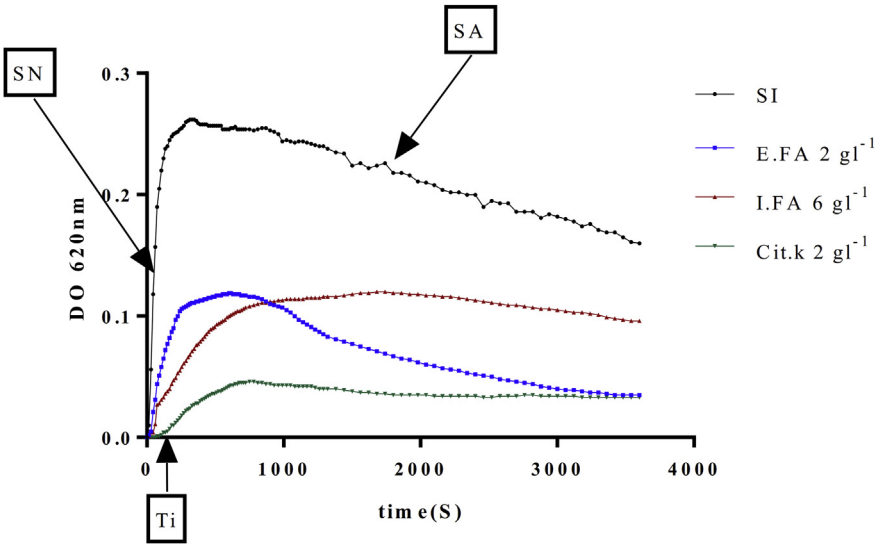

Fig. 2. The temporal evolution of the optical density in absence (SI) and in the presence of I.FA; E.FA and the solution of Cit.K (n = 3). E.FA: hydroalcoholuc extract of *A. unedo*, I.FA: infusion of *A. unedo*, Cit.K: potassium citrate, SI: absence of inhibitor, SN: slopes of nucleation, SA: slopes of aggregation, Ti: induction time.

efficiency of I.FA in inhibiting the gathering of crystalline nuclei that can form aggregates.

3.4. Inhibition of the calcium oxalate's crystallization

The induction time (Ti) values in the presence and in the absence of the different concentrations of inhibitors: E.FA and I.FA are shown in Fig. 3.

The interpretation of Fig. 3 exhibits that the induction time Ti in the presence of E.FA and I.FA is shorter compared to Ti in the presence of Cit.K taken as a

https://doi.org/10.1016/j.heliyon.2018.e01011

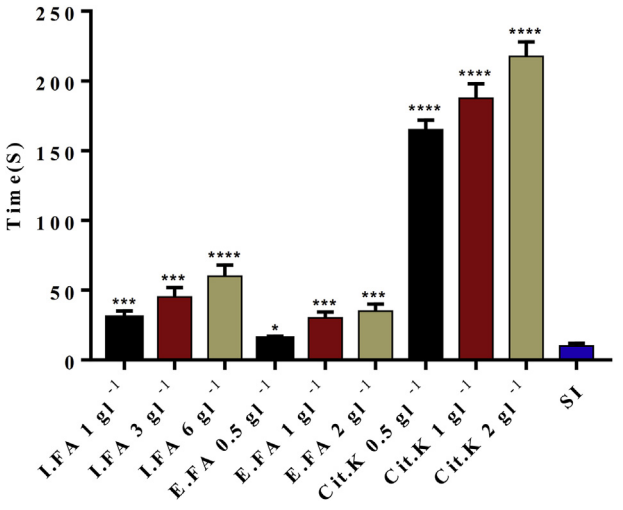

Fig. 3. Induction time, in the presence and absence of inhibitors. Values are expressed as mean ± SD ($n = 3$). E.FA: hydroalcoholic extract of *A. unedo*, I.FA: infusion of *A. unedo*, Cit.K: potassium citrate, SI: absence of inhibitor.
*p < 0.05; **p < 0.01; ***p < 0.005; ****p < 0.001 vs. absence of inhibitor.

reference, with values of 60; 34; 217 and 10 s for I.FA; E FA; Cit. K and SI respectively. In this respect, the value of Ti undergoes a slight increase compared to the increase in the concentration regardless of the extract studied. Indeed, the Ti values are 15, 30 and 35 s for E.FA concentrations of 0.5, 1 and 2 gl^{-1} respectively and 30, 45 and 60 s for I.FA concentrations of 1, 3 and 6 gl^{-1} respectively. While the values of Ti goes from 165 to 217 s, the concentration of Cit.K goes from 0.5 to 2 gl^{-1}.

Moreover, the crystallization inhibition potential in the presence of different concentrations of I.FA, E.FA and Cit.K in the stages of nucleation and aggregation have been calculated from the comparison of the slopes of the latter by the slopes of the test without inhibitor. The results are displayed in Tables 2 and 3 respectively.

Table 2. Percent inhibition of nucleation in the presence of I.FA, E.FA and the solution of Cit.K.

	Inhibitor								
	I.FA			**E.FA**			**Cit.K**		
Concentration (gl^{-1})	**1**	**3**	**6**	**0.5**	**1**	**2**	**0.5**	**1**	**2**
%inhibition	11.76 ±0.035 ****	13.35 ±0.12 ****	69.41 ±0.24 ****	-34.78 ±0.97 ***	-24.3 ±0.29 ***	19.76 ±0.27 **	96.52 ±0.01	97.01 ±0.06	97.37 ±0.16
R	0.95	0.97	0.95	0.97	0.97	0.95	0.97	0.99	0.99
CV	2.35	7.75	4.23	7.19	9.75	7.05	0.3	0.2	6

Values are expressed as mean ± SD ($n = 3$). E.FA: hydroalcoholic extract of *A. unedo*, I.FA: infusion of *A. unedo*, Cit.K: potassium citrate, R: correlation coefficient, CV: variation coefficient.
*p < 0.05 **p < 0.01 ***p < 0.005 ****p < 0.001 vs. Potassium Citrate.

https://doi.org/10.1016/j.heliyon.2018.e01011

Table 3. Percent inhibition of aggregation in the presence of I.FA, E.FA and the solution of Cit.K.

	Inhibitor								
	I.FA			**E.FA**			**Cit.K**		
Concentration (gl^{-1})	**1**	**3**	**6**	**0.5**	**1**	**2**	**0.5**	**1**	**2**
%inhibition	41.66 ± 1.83***	72.35 ± 1.14**	93.92 ± 2.61***	34.67 ± 2.78***	43.98 ± 3.06***	45.16 ± 3.02****	68.25 ± 2.40	69,70 ± 2.85	77,12 ± 2.16
R	0.99	0.95	0.96	0.96	0.97	0.95	0.97	0.95	0.95
CV	5.02	6.61	6.76	8.81	8.93	9.49	7.9	9.4	9.4

Values are expressed as mean ± SD ($n = 3$). E.FA: hydroalcoholic extract of *A. unedo*, I.FA: infusion of *A. unedo*, Cit.K: potassium citrate, R: correlation coefficient, CV: variation coefficient.
*p < 0.05 **p < 0.01 ***p < 0.005 ****p < 0.001 vs. Potassium Citrate.

The percentages of nucleation inhibition for I.FA are significantly lower compared to Cit.K. Indeed, they are in the order of 11.76 ± 0.035 to 69.41 ± 0.024% and of 96.52 ± 0.01 to 97.37 ± 0.16% for concentrations of 1 to 6 gl^{-1} and 0.5 to 2 gl^{-1} respectively, with R greater than 0.95 and CV lower than 10% for both. On the other hand, the negative values of the inhibition rate for E.FA which are from -34.78 ± 0.97 to 19.76 ± 0. 27% for concentrations of 0.5 to 2 gl^{-1} respectively (with; $R \geq 0.95$ and $CV \leq 10$) show that the latter has no significant effect on the inhibition of nucleation.

The analysis of the aggregation potential values given in Table 3 shows that the best inhibition rate corresponds to the treatment with I.FA with values of 41.66 ± 1.83, 72.35 ± 1.14 and 93.92 ± 2.61%, for concentrations from 1; 3 and 6 gl^{-1} respectively. Additionally, the inhibition rate for Cit.K is in the order of 68.25 ± 2.40, 69.70 ± 2.85% at 77.12 ± 2.16% for concentrations of 0.5, 1 and 2 gl^{-1} respectively (with; $R \geq 0.95$ and $CV \leq 10$). As for E.FA, the values are 34.67 ± 2.78%; 43.98 ± 3.06 and 45.16 ± 3.02 for concentrations of 0.5, 1 and 2 gl^{-1} respectively (with; $R \geq 0.95$ and $CV \leq 10$).

3.5. Microscopic observation

In order to validate our outcomes achieved by the spectrophotometric model, the rate of aggregates has been calculated from the observation of the samples placed in a Malassez cell; containing the crystals and/or aggregates every ten min, for the concentrations that gave the best inhibition rates which are 2 gl^{-1} for E.FA and Cit.K and 6 gl^{-1} for I.FA. Hence, the results obtained are shown in Table 4.

The results exhibited in Table 4 show the existence of aggregates after 10 min which represents the nucleation phase on the one hand and the rate of aggregates is greater in the case without inhibitor and whatever is the time studied on the other hand.

https://doi.org/10.1016/j.heliyon.2018.e01011

Table 4. Aggregates percentage.

Time (min)	Aggregates Percentage (%)			
	S.I	I.FA	E.FA	Cit.K
10	32.33 ± 2.25	8.00 ± 3.42**	28.13 ± 6.50**	5.66 ± 2.33*
20	32.61 ± 4.56	12.00 ± 3.22***	36,68 ± 8.54*	10.94 ± 2.32**
30	32.95 ± 5.91	18.12 ± 3.84****	48,69 ± 8.82*	12.87 ± 3.82*
40	36.80 ± 4.61	11.83 ± 4.93*	56,61 ± 9.32**	23.60 ± 3.36***
50	38.31 ± 5.39	10.74 ± 4.09**	43,84 ± 7.75***	19.29 ± 5.05****
60	51.15 ± 3.67	9.97 ± 4.52**	32,60 ± 8.03	17.64 ± 3.72**

Values are expressed as mean ± SD ($n = 3$). E.FA: hydroalcoholic extract of *A. unedo*, I.FA: infusion of *A. unedo*, Cit.K: potassium citrate, SI: absence of inhibitor.
*p < 0.05 **p < 0.01 ***p < 0.005 ****p < 0.001 vs. absence of inhibitor.

During the nucleation phase, Cit.K remains the best inhibitor of aggregate formation with a value of 5.66 ± 2.33% against 8.00 ± 3.42 and 28.13 ± 6.50% for I.FA and E.FA respectively. On the other hand, the analysis of the values given in Table 4 for a time greater than 30 minutes, which corresponds to the aggregation phase, explains the fact that treatment with I.FA is more effective than even treatment with Cit.K. In fact, the percentage of aggregates at 30, 40 and 60 minutes are 18.12 ± 3.84, 11.83 ± 4.93, 9.97 ± 4.52% for I.FA and 12.87 ± 3.82, 23.60 ± 3.36 and 17.64 ± 3.72% for Cit.K.

Images allowing to following the appearance and shape of the crystals during the nucleation phase as well as the volume of the aggregates during the aggregation phase have been recorded using an optical microscope for the different inhibitors studied, and are shown in Figs. 4 and 5 respectively.

The analysis of the four images related to the nucleation phase (Fig. 4) reveals the presence of aggregates in addition to a predominance of the crystals. In this case, the amount of these is less important in the case of inhibition by Cit.K. However, this result is in perfect agreement with the calculated aggregate rate.

The analysis of the images related to the aggregation phase displays the presence of larger and more numerous aggregates, especially in the case without inhibitor S.I. Besides, the comparison of the four images in Fig. 5 shows that the size of the latter decreases and that the number becomes less important especially in the case of treatment with I.EA and then Cit.K. This result can be demonstrated by the inhibition of growth and crystalline aggregation by the polyphenols contained in the plant or by the dissociation of aggregates by bioactive molecules of the extracts. The same explanation has been given by Daudon *et al.* [36]. Thus, these results confirm the validity of our spectrophotometric method.

https://doi.org/10.1016/j.heliyon.2018.e01011

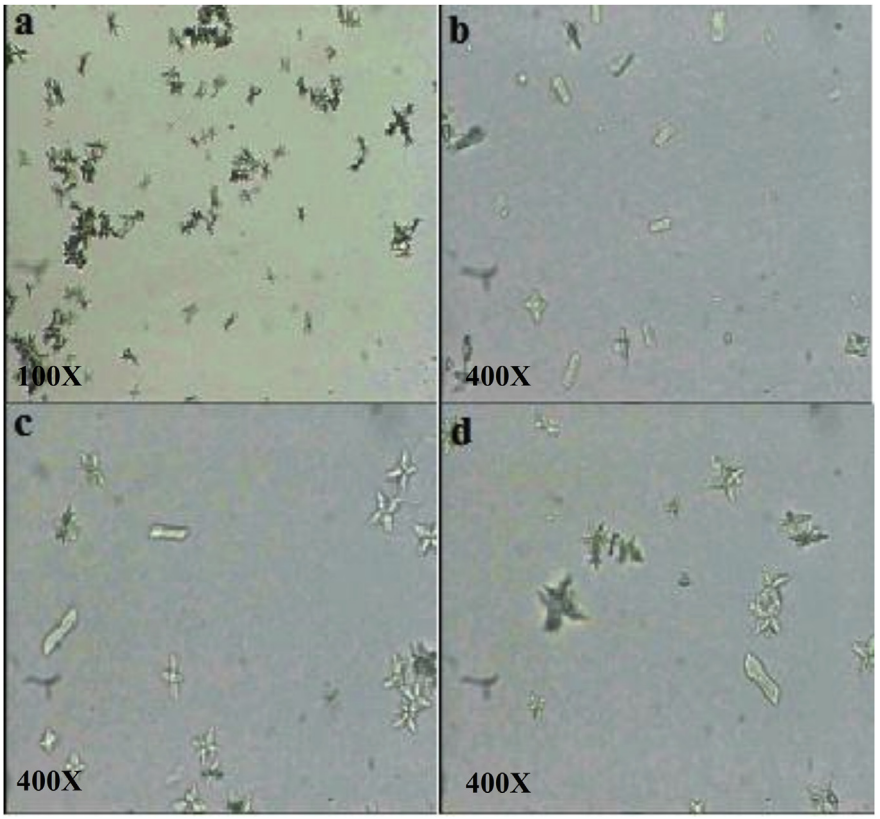

Fig. 4. Crystals of calcium oxalate. a: SI; b: I.FA; c: Cit.K; d: E.FA. E.FA: hydroalchoholic extract of *A. unedo*, I.FA: infusion of *A. unedo*, Cit.K: potassium citrate, SI: absence of inhibitor.

3.6. Characterization of crystals

The crystals synthesized in the absence and in the presence of different concentrations of I.FA and E.FA have been characterized by Fourier Transform Infrared Spectroscopy (FT-IR), in order to determine both their chemical constitution and their transformation in terms of their type; hence, the spectra obtained are shown in Fig. 6.

According to Fig. 6, in the case of the absence of inhibitor (Fig. 6a), two bands at 3509 and 3429 cm^{-1} are critical to OH stretching of the water, an out-of-plane C-O deformation band [37], and another bending O-C-O plane [38] have been observed at 782 and 515 cm^{-1} respectively. However, absorption bands have been noticed at 1671/1619 cm^{-1} and 1383/1325 cm^{-1}; the former are attributing to the antisymmetric carbonyl stretching band (vas (COO-)), the second are compatible with the symmetrical stretching band of the metal-carboxylate (vs (COO-)); these bands are corresponding to COT crystals [38, 39, 40, 41].

On the contrary, in the presence of E.FA with concentrations of 0.5; 1 and $2g^{-1}$ (Fig. 6b, c and d), multiple bands are observed between 3060 and 3600 cm^{-1} critical

https://doi.org/10.1016/j.heliyon.2018.e01011

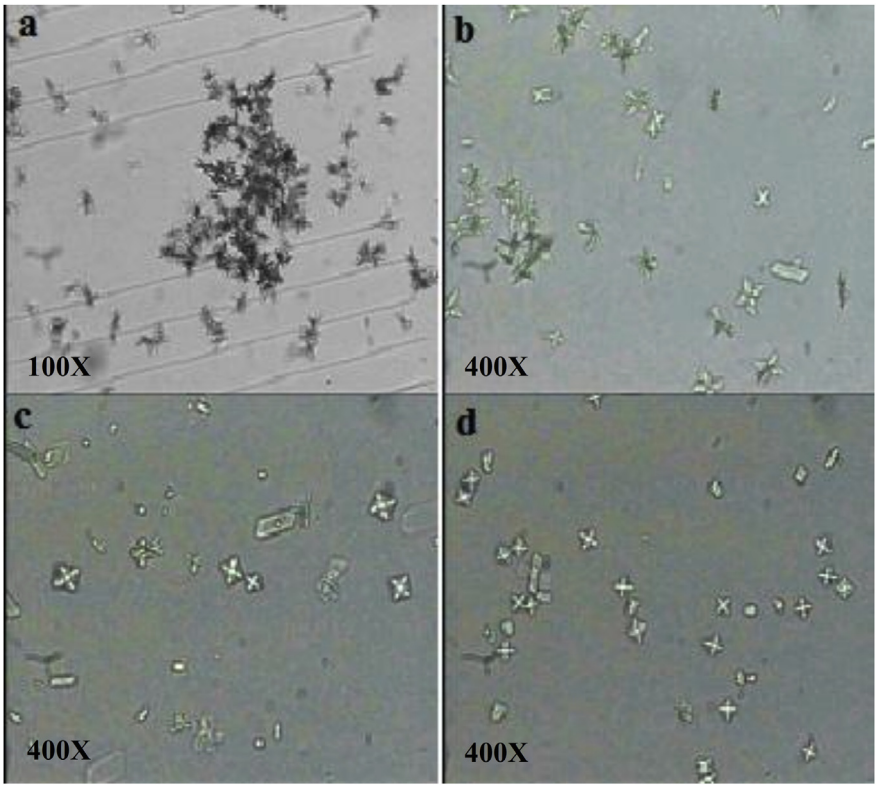

Fig. 5. Aggregates of calcium oxalate crystals. a: SI; b: I.FA; c: Cit.K; d: E.FA. E>FA: hydroalcoholic extract of *A. unedo*, I.FA: infusion of *A. unedo*, Cit.K: potassium citrate, SI: absence of inhibitor.

to the OH stretching of the water, and corresponding to COM crystals in addition to the presence of a sharp plane bending band at 782 ± 3. The existence of bands at 652 ± 2 and 550 ± 3 cm^{-1} and absorption bands (vas (COO-)) at 1674/1617 cm^{-1} and (vs (COO-)) at 1382/1325 cm^{-1} confirms the formation of COT crystals [40, 41]. On the other hand, in the presence of different concentrations of I.FA (Fig. 6f and g), it is inferred that a single absorption peak between 3456 ± 2 cm^{-1} asserts the presence of the COD crystals [42], in addition a bending band out of the water at 782 ± 2 cm^{-1} [43]. In this case, two bands of absorptions have been observed at 1642 cm^{-1} for (vas (COO-)) and 1328 cm^{-1} for (vs (COO-)) attest the formation of COD [41, 44]. Moreover, the presence of absorption peak at 1630 cm^{-1} and another at 649 $cm\text{-}^{1}$ in the case where the concentration of I.FA is 1 g^{-1}(Fig. 6e) can signify a mixture between the crystals of COD and COM.

4. Discussion

The braking of the stones growth in the first stages of crystallization, which are the nucleation and the aggregation, remains the main concern of the doctors especially for the patients who recidivate. The model of turbidimetric crystallization without

https://doi.org/10.1016/j.heliyon.2018.e01011

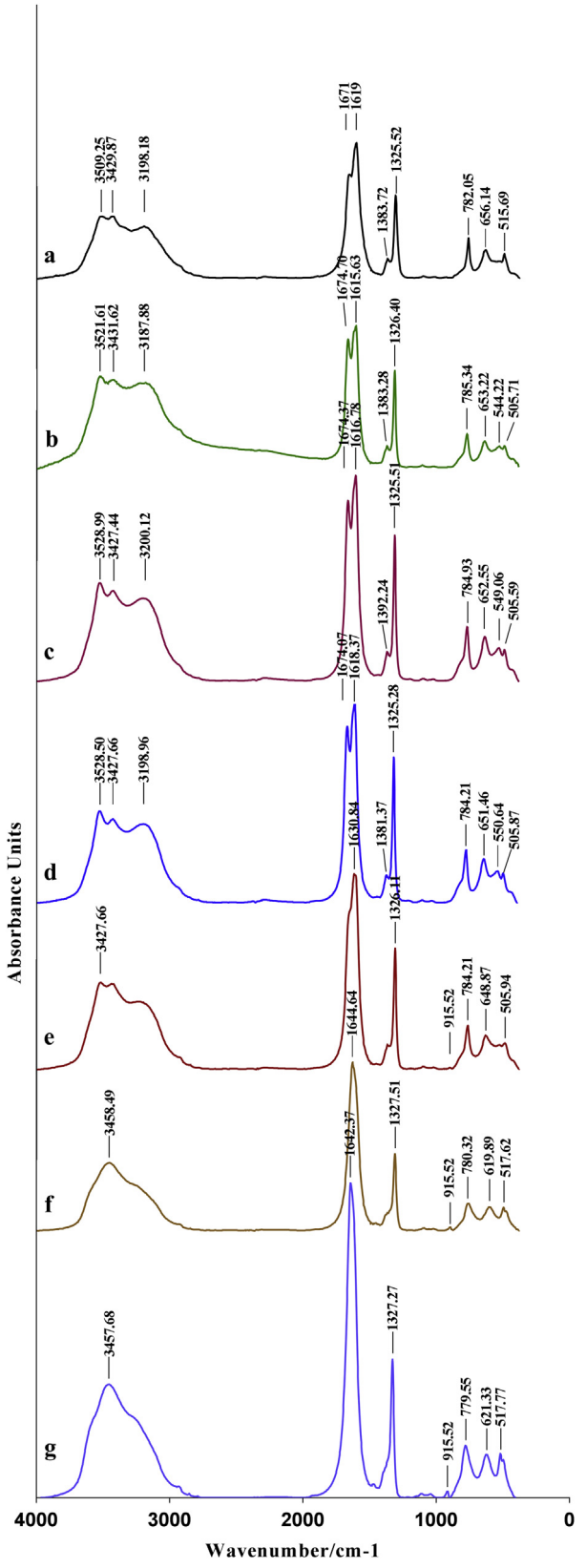

https://doi.org/10.1016/j.heliyon.2018.e01011

(SI) and in the presence of inhibitors of E.FA and I.FA, makes it possible to follow both the various steps of the crystallization and to determine the kinetic parameters, in particular the induction time (Ti) which corresponds to the time necessary for the formation of the first stable and detectable crystal nucleus by the UV-Visible spectrophotometer. The outcomes found well explained that the plant is not involved in a huge way in the delay in the crystal formation compared to potassium citrate. Furthermore, the increase in the value of Ti signifies the delay of crystalline nucleation [45]. Consequently, this delay in Ti may be related not only to the delay in nucleation of detectable particles, but also to the presence of an increased rate of nucleation of very small particles that are undetectable [32].Yet, the inhibition's rate of nucleation varies depending on the concentration and the type of extract, the results obtained prove that I.FA more effective but remains less important when compared with the Cit.k. On the other hand, our results of I.FA far exceed the results of the works of Khan *et al.* [46], who found values of 10 $\pm$ 1.73 20 $\pm$ 1.7% for concentrations of 0.5 to 2 gl^{-1} with the hydro-methanolic extract of Origanum vulgare. In addition, they approach those of Rajeshwari et al. [47] and Saranya and Geetha [48], who worked on the infusion of the Convolvulus arvensis flowers and on the aqueous extract of the roots Beta vulgaris L. respectively. So, that hess *et al* [32] found negative values of nucleation inhibition by albumin.

The importance of the aggregation rate determination lies in the estimation of the lithogenic potential and in the evaluation of the therapeutic measures effectiveness intended to reduce the risk of recurrence [49]. However, the comparison of the inhibition effects of crystallization in the two stages for the two extracts display that I.FA is more effective than Cit.k especially in the inhibition of aggregation. For this reason, this result can be explained by the presence of polar compounds in extracts such as polyphenols in the plant (Table 1). Indeed, these have an anti-crystallising effect according to studies made on both human urine as well as on animal models [50]. However Noorafshan *et al.* [51] have been reported that Diosmin which is a flavonoid prevents CaC_2O_4 deposition on crystals. The contradictory effect of E.FA in the two steps of the crystallization of calcium oxalate, can be explained by the fact that the two steps are not independent, and that the compounds of the extract are fixed on the surface of the crystalline nuclei preventing the development of the aggregate [32]. On the other hand, the characterization of the crystals shows a high efficiency of I.FA in the inhibition of the formation of COT and COM crystals. The latter has a high affinity for renal tubular cells as DOC crystals that are almost neutral on the surface [52], and consequently the prevention of aggregation.

Fig. 6. FT-IR spectra of the synthesized crystals. a: SI; b: E.FA 0.5 gl^{-1}; c: E.FA 1 gl^{-1}; d: E.FA 2 gl^{-1}; e: I.FA 1 gl^{-1}; f: I.FA 3 gl^{-1}; I.FA 6 gl^{-1}. SI: absence of inhibitor, E.FA: hydroalcoholic extract of *A. unedo*, I.FA: infusion of *A. unedo*.

https://doi.org/10.1016/j.heliyon.2018.e01011

In conclusion, *A. unedo* has been valued in the treatment of lithiasis and the prevention of the calcium oxalate's crystals formation. For this reason two different extracts have been prepared one by infusion and the other using a Soxhlet montage and then analyzed qualitatively to reveal their composition in large chemical families. These have been tested in attenuation of calcium oxalate crystal formation by the turbiditymetry method compared with tests performed with Cit.K. The objective of this work is to approach the big chemical family responsible for this phenomenon. Comparing the tests of the two extracts with potassium citrate concluded a slightly inferior efficacy of the infusion *A. unedo* in the nucleation stage and more important in the stage of aggregation. Indeed, the rate of inhibition of crystallization by the infusion in the aggregation phase is in the order of $93.92 \pm 2.61\%$ for a concentration equal to 6 gl^{-1} and $77.12 \pm 2.16\%$ for an equal concentration at 2 gl^{-1} for the Cit.K. Microscopic observation confirms these results, as well as the validity and reproducibility of the spectrophotometric method. However, *in vivo* studies on animal models are needed and are intended to judge its potential therapeutic values of the plant.

Declarations

Author contribution statement

Rabie Kachkoul: Conceived and designed the experiments; Performed the experiments; Analyzed and interpreted the data; Wrote the paper.

Tarik Sqalli Houssaini 13: Conceived and designed the experiments; Analyzed and interpreted the data.

Radouane El Habbani, Youssef Miyah, Mohamed Mohim: Performed the experiments.

Anissa Lahrichi: Conceived and designed the experiments; Analyzed and interpreted the data; Contributed reagents, materials, analysis tools or data; Wrote the paper.

Funding statement

This research did not receive any specific grant from funding agencies in the public, commercial, or not-for-profit sectors.

Competing interest statement

The authors declare no conflict of interest.

Additional information

No additional information is available for this paper.

https://doi.org/10.1016/j.heliyon.2018.e01011

Acknowledgements

The authors thank Professor: Amina BARI (Department of Biology. Faculty of sciences Dhar Mahraz, university Sidi Mohammed Ben Abdellah Fèz, Morocco) for the identification of the plant.

References

[1] A.C. Pizzato, E.J.G. Barros, Dietary calcium intake among patients with urinary calculi, Nutr. Res. 23 (2003) 1651−1660.

[2] A. Hesse, E. Brandle, D. Wilbert, K.-U. Kohrmann, P. Alken, Study on the prevalence and incidence of urolithiasis in Germany comparing the years 1979 vs. 2000, Eur. Urol. 44 (2003) 709−713.

[3] M. El Khebir, O. Fougeras, C. Le Gall, A. Santin, C. Perrier, C. Sureau, J. Miranda, P. Ecollan, G. Bagou, A. Trinh-Duc, O. Traxer, Actualisation 2008 de la 8e Conférence de consensus de la Société francophone d'urgences médicales de 1999. Prise en charge des coliques néphrétiques de l'adulte dans les services d'accueil et d'urgences, Prog. Urol. 19 (2009) 462−473.

[4] M. Daudon, Épidémiologie actuelle de la lithiase rénale en France, Ann. Urol. 39 (2005) 209−231.

[5] V. Castiglione, F. Jouret, O. Bruyére, B. Dubois, T. Thomas, D. Waltregny, A.-C. Bekaert, E. Cavalier, Épidémiologie de la lithiase urinaire en Belgique sur base d'une classification morpho-constitutionnelle, Nephrol. Ther. 11 (2015) 42−49.

[6] K.K. Stamatelou, M.E. Francis, C.A. Jones, L.M. Nyberg, G.C. Curhan JR., Time trends in reported prevalence of kidney stones in the United States: 1976−1994, Kidney Int. 63 (2003) 1817−1823.

[7] R. El Habbani, A. Chaqroune, T. Sqalli Houssaini, M. Arrayhani, J. El Ammari, F. Dami, B.A. Chouhani, A. Lahrichi, Étude épidémiologique sur les calculs urinaires dans la région de Fès et sur le risque de récidive, Prog. Urol. 26 (5) (2016) 287−294.

[8] J.A. Wesson, E.M. Worcester, J.M. Wiessenter, N.S. Mandel, J.G. Kleinman, Control of calcium oxalate crystal structure and cell adherence by urinary macromolecules, Kidney Int. 53 (1998) 952−957.

[9] C.F. Verkoelem, J.C. Romijn, W.C. De Bruin, E.R. Boeve, L.-C. Cao, F.H. Schroder, Association of calcium oxalate monohydrate crystals with MDCK cells, Kidney Int. 48 (1995) 129−138.

https://doi.org/10.1016/j.heliyon.2018.e01011

[10] A. Khouchlaa, M. Tijane, A. Chebat, S. Hseini, A. Kahouadji, Ethnopharmacology Study of Medicinal Plants Used in the Treatment of Urolithiasis (Morocco), Phytothérapie, 2016.

[11] N. Tahri, A. EL Basti, L. Zidane, A. Rochdi, A. Douira, Etude ethnobotanique des plantes medicinales dans La province De Settat (Maroc), J. For. Fac Kastam Univ. 12 (2) (2012) 192−208.

[12] K. Mikou, S. Rachiq, A. Jarrar Oulidi, G. Beniaich, Ethnobotanical Survey of Medicinal and Aromatic Plants Used by the People of Fez in Morocco, Phytothérapie, 2015.

[13] M. Ghourri, L. Zidane, A. Douira, Catalogue des plantes médicinales utilisées dans le traitement de la lithiase rénale dans la province de Tan-Tan (Maroc saharien), Int. J. Biol. Chem. Sci. 7 (4) (2013) 1688−1700.

[14] J. El-Hilaly, M. Hmammouchi, B. Lyoussi, Ethnobotanical studies and economic evaluation of medicinal plants in Taounate province (Northern Morocco), J. Ethnopharmacol. 86 (2003) 149−158.

[15] M. Leonti, L. Casu, F. Sanna, L. Bonsignore, A comparison of medicinal plant use in Sardinia and Sicily-De Materia Medica revisited, J. Ethnopharmacol. 12 (2009) 255−267.

[16] A. Ziyyat, E.-H. Boussairi, Cardiovascular effects of *Arbutus unedo* L. in spontaneously hypertensive rats, Phytother Res. 12 (1998) 110−113.

[17] S. Afkir, T.B. Nguelefack, M. Aziz, J. Zoheir, G. Cuisinaud, M. Bnouham, H. Mekhfi, A. Legssyer, S. Lahlou, A. Ziyyat, Arbutus unedo prevents cardiovascular and morphological alterations in L-NAME-induced hypertensive rats Part I: cardiovascular and renal hemodynamic effects of Arbutus unedo in L-NAME-induced hypertensive rats, J. Ethnopharmacol. 116 (2008) 288−295.

[18] A. Ziyyat, H. Mekhfi, M. Bnouham, A. Tahri, A. Legssyer, J. Hoerter, R. Fischmeister, *Arbutus unedo* induces endothelium-dependent relaxation of the isolated rat aorta, Phytother. Res. 16 (2002) 572−575.

[19] H.H. Orak, H. Yagar, S.S. Isbilir, A.S. Demirci, T. Gümüş, N. Ekinci, Evaluation of antioxidant and antimicrobial potential of strawberry tree (*Arbutus unedo* L.) leaf, Food Sci. Biotechnol. 20 (5) (2011) 1249−1256.

[20] I. Moualek, G.I. Aiche, N.M. Guechaoui, S. Lahcene, K. Houali, Antioxidant and anti-inflammatory activities of *Arbutus unedo* aqueous extract, Asian Pac J Trop Biomed 6 (11) (2016) 937−944.

[21] G. Celikel, L. Demirsoy, H. Demirsoy, The strawberry tree (*Arbutus unedo* L.) selection in Turkey, Sci. Hortic. 118 (2008) 115−119.

 https://doi.org/10.1016/j.heliyon.2018.e01011

[22] M. Virot, V. Tomao, C. Ginies, F. Visinoni, F. Chemat, Green procedure with a green solvent for fats and oils' determination Microwave-integrated Soxhlet using limonene followed by microwave Clevenger distillation, J. Chromatogr. A 1196−1197 (2008) 147−152.

[23] S. Feknous, F. Saidi, M.R. Said, Extraction, caractérisation et identification de quelques metabolites secondaires actifs de la mélisse (*Melissa officinalis* L.), Nat. Technol. 11 (2014) 7−13.

[24] A. Jiménez-Zamora, C. Delgado-Andrade, J.A. Rufián-Henares, Antioxidant capacity, total phenols and color profile during the storage of selected plants used for infusion, Food Chem. 199 (2016) 339−346.

[25] K. N'Guessan, B. Kadja, G.N. Zirihi, D. Traoré, L. Aké-assi, Screening phytochimique de quelques plantes médicinales ivoiriennes utilisées en pays Krobou (Agboville, Côte-d'Ivoire), Sci. Nat. 6 (1) (2009) 1−15.

[26] A.J. Harborne, Phytochemical Methods a Guide to Modern Techniques of Plant Analysis, Springer Science et Business Media, 1998.

[27] N. Ghedadba, L. Hambaba, A. Ayachi, M.C. Aberkane, H. Bousselsela, S.M. Oueld-Mokhtar, Polyphénols totaux, activités antioxydante et antimicrobienne des extraits des feuilles de Marrubium deserti de Noé, Phytothérapie 13 (2) (2015) 118−129.

[28] A.M. Khan, R.A. Qureshi, F. Ullah, S.A. Gilani, A. Nosheen, S. Sahreen, M.K. Laghari, M.Y. Laghari, S-Ur-. Rehman, I. Hussain, W. Murad, Phytochemical analysis of selected medicinal plants of Margalla Hills and surroundings, J. Med. Plants Res. 5 (25) (2011) 6017−6023.

[29] E. Iqbal, K. Abu Salim, L.B.L. Lim, Phytochemical screening, total phenolics and antioxidant activities of bark and leaf extracts of *Goniothalamus velutinus* (Airy Shaw) from Brunei Darussalam, J. King Saud Univ. Sci. 27 (2015) 224−232.

[30] V.L. Singleton, J.A. Rossi Jr., Colorimetry of total phenolics with phosphomolybdic−phosphotungstic acid reagents, Am. J. Enol. Vitic. 16 (1965) 144−158.

[31] K.W. Kong, S. Mat-Junit, N. Aminudin, A. Ismail, A. Abdul-Aziz, Antioxidant activities and polyphenolics from the shoots of *Barringtonia racemosa* (L.) Spreng in a polar to apolar medium system, Food Chem. 134 (2012) 324−332.

[32] B. Hess, U. Meinhardt, L. Zipperle, R. Giovanoli, P. Jaeger, Simultaneous measurements of calcium oxalate crystal nucleation and aggregation: impact of various modifiers, Urol. Res. 23 (1995) 231−238.

https://doi.org/10.1016/j.heliyon.2018.e01011

[33] R. Kachkoul, T. Sqalli Houssaini, Y. Miyah, M. Mohim, R. El Habbani, A. Lahrichi, The study of the inhibitory effect of calcium oxalate monohydrate's crystallization by two medicinal and aromatic plants: *Ammi visnaga* and *Punica granatum*, Prog. Urol. 28 (2018) 156−165.

[34] B. Hess, S. Jordi, L. Zipperle, E. Ettinger, R. Giovanoli, Citrate determines calcium oxalate crystallization kinetics and crystal morphology-studies in the presence of Tamm-Horsfall protein of a healthy subject and a severely recurrent calcium stone former, Nephrol. Dial. Transplant. 15 (2000) 366−374.

[35] H.N. Mrabti, I. Marmouzi, K. Sayah, L. Chemla, Y. El Ouadi, H. Elmsellem, Y. Cherrah, M.A. Faouzi, *Arbutus unedo* L. aqueous extract is associated with *in vitro* and *in vivo* antioxidant activity, JMESJ 8 (1) (2017) 217−224.

[36] M. Daudon, O. Traxerb, E. Lechevallier, C. Saussine, La lithogenèse, Prog. Urol. 18 (2008) 815−827.

[37] T.H.-S. Hsu, S.Y. Lin, C.-C. Lin, W.T. Cheng, Preliminary feasibility study of FTIR microscopic mapping system for the rapid detection of the composited components of prostatic calculi, Urol. Res. 39 (2011) 165−170.

[38] J.M. Ouyang, H. Zheng, S.-P. Deng, Simultaneous formation of calcium oxalate (mono-, di-, and trihydrate) induced by potassium tartrate in gelatinous system, J. Cryst. Growth 293 (2006) 118−123.

[39] J.M. Ouyang, N. Zhou, L. Duan, B. Tieke, Ability of multifunctional sodium carboxylates to favor crystal growth of calcium oxalate dihydrate and trihydrate in lecithin-water liposome systems, Colloids Surf. A. 245 (2004) 153−162.

[40] J.M. Ouyang, S.-P. Deng, N. Zhou, B. Tieke, Effect of tartrates with various counterions on the precipitation of calcium oxalate in vesicle solutions, Colloids Surf. A. Eng. Aspects 256 (2005) 21−27.

[41] C. Conti, M. Casati, C. Colombo, E. Possenti, M. Realini, G.D. Gatta, M. Merlini, L. Brambilla, G. Zerbi, Synthesis of calcium oxalate trihydrate: new data by vibrational spectroscopy and synchrotron X-ray diffraction, Spectrochim. Acta A. 150 (2015) 721−730.

[42] Y. Xiu-Qiong, O. Jian-Ming, P. Hua, Z. Wen-Yu, C. He-Qun, Inhibition on calcium oxalate crystallization and repair on injured renal epithelial cells of degraded soybean polysaccharide, Carbohydr. Polym. 90 (2012) 392−398.

[43] Y. Zhang, Y. Tang, J. Xu, D. Zhang, G. Lu, W. Jing, Modulation of polyepoxysuccinic acid on crystallization of calcium oxalate, J. Solid State Chem. 231 (2015) 7−12.

https://doi.org/10.1016/j.heliyon.2018.e01011

[44] J.M. Ouyang, L. Duan, B. Tieke, Effects of carboxylic acids on the crystal growth of calcium oxalate nanoparticles in lecithin-water liposome systems, Langmuir 19 (2003) 8980−8985.

[45] C. Hennequin, V. Lalanne, M. Daudon, B. Lacour, T. Drueke, A new approach to studying inhibitors of calcium oxalate crystal growth, Urol. Res. 21 (1993) 101−108.

[46] A. Khan, S. Bashir, S. R Khan, A.H. Gilani, Antiurolithic activity of *Origanum vulgare* ismediated through multiple pathways, BMC Complement Altern. Med. 11 (2011) 96.

[47] P. Rajeshwari, G. Rajeswari, S.K. Jabbirulla, IV. Vardhan, evaluation of *in vitro* anti-urolithiasis activity of *Convolvulus arvensis*, Int. J. Pharm. Pharmaceut. Sci. 5 (3) (2013) 599−601.

[48] R. Saranya, N. Geetha, Inhibition of calcium oxalate (caox) crystallization in vitro by the extract of beet root (*Beta vulgaris* L), Int. J. Pharm. Pharmaceut. Sci. 6 (2) (2014) 361−3361.

[49] M. Daudon, Cristallurie, Nephrol. Ther. 11 (3) (2015) 174−190.

[50] Y.S. Zhong, C.H. Yu, H.Z. Ying, Z.Y. Wang, H.F. Cai, Prophylactic effects of *Orthosiphon stamineus* Benth. Extracts on experimental induction of calcium oxalate nephrolithiasis in rats, J. Ethnopharmacol. 144 (2012) 761−767.

[51] A. Noorafshan, S.K. Doust, F. Karimi, Diosmin reduces calcium oxalate deposition and tissue degeneration in nephrolithiasisin rats: a stereological study, Korean J Urol 54 (2013) 252−257.

[52] J.M. Ouyang, M. Wang, P. Lu, J. Tan, Degradation of sulfated polysaccharide extracted from algal *Laminaria japonica* and its modulation on calcium oxalate crystallization, Mater. Sci. Eng. C 30 (2010) 1022−1029.

https://doi.org/10.1016/j.heliyon.2018.e01011